Supporting Information for Publication

Rational integration of photovoltaics for solar hydrogen generation

Dr Fiona J Beck*,

Research School of Electrical, Energy and Materials Engineering, Australian National University, Ian Ross Building, 31 North Road, Acton, ACT, 2601, Australia

*[*fiona.beck@anu.edu.au](mailto:fiona.beck@anu.edu.au)*

Efficiency models

For an ideal PV component, all incident photons in the solar spectra with energies above the semiconductor bandgap energy, E_g, are absorbed and contribute to the photocurrent, calculated as

$$j_L = e \int_{\lambda_{min}}^{\frac{hc}{Eg}} \Phi(\lambda) d\lambda, \qquad (1)$$

where $\Phi(\lambda)$ is the wavelength dependent photon flux of the standard solar spectrum (AM 1.5g), c is the speed of light, λ is the wavelength of light, e is the charge on the electron, and h is Planck's constant. The only loss that is considered is blackbody radiation from the cell at room temperature, in the form of the radiative recombination current density:

$$j_{rad} = e \int_{\lambda_{min}}^{\frac{hc}{Eg}} \frac{2\pi c}{\lambda^4} \left(exp\left[\frac{hc}{\lambda k_B T}\right] - 1 \right) d\lambda, \qquad (2)$$

where k_B is the Boltzmann constant and T is the temperature of the semiconductor. The current density dependent photovoltage of the cell is then given by:

$$V_{PV}(j) = \frac{k_B T}{e} ln \left(\frac{j_L - j}{j_{rad}} + 1 \right). \qquad (3)$$

The maximum power density that can be provided by a PV cell is given by

$$MPP = \max_{0 \leq j \leq j_L} V_{PV}(j)j. \qquad (4)$$

This is known as the maximum power point, and is used to calculate the optimum efficiency of the PV cell:

$$\eta_{PV} = \frac{MPP}{P_{AM1.5g}}, \qquad (5)$$

where the solar power density is calculated as

$$P_{AM1.5g} = \int_{AM1.5g} \frac{hc}{\lambda} \Phi(\lambda) d\lambda, \qquad (6)$$

To drive electrochemical water splitting, the input voltage, $V_{IN}(j)$, must be large enough to overcome the potential of the reaction ($\Delta E = 1.23V$ for water splitting), and any additional voltage losses introduced by the catalysts and by resistance to charge transport. This can be written as:

$$V_{IN}(j) \geq \Delta E + V_{OER}(j) + V_{HER}(j) + V_e(j), \tag{7}$$

where j is the current density through the electrochemical circuit. We follow the approach of Fountaine and colleagues[1,2] and use Butler-Volmer kinetics[3] to model the over-potential of the catalysts

$$V_{OER/HER}(j) = \frac{RT}{\alpha n_e F} sinh^{-1}\left(\frac{j}{2 j_{OER/HER}}\right), \tag{8}$$

where R is the universal gas constant, F is the Faraday constant, and $n_e = 2$ is the number of electrons involved in the reaction. The catalytic exchange current density, $j_{OER/HER}$ and the charge transfer coefficient, α, are both specific to a given catalyst and are generally empirically determined. This formulation implicitly assumes that the forward and reverse charge transfer coefficients are equal: $\alpha_F = \alpha_R = \alpha$.

Additional voltage losses due to ionic transport through the system are given by:

$$V_e(j) = jR_e, \tag{9}$$

where R_e is the resistance of the electrolyte. Any other resistance losses due to transport anywhere else in the system can be included with additional Ohmic terms but are neglected here.

The power-to-hydrogen efficiency of an electrochemical cell is defined, relative to the input power, P_{IN} by

$$\eta_{PTH} = \frac{j \Delta E \eta_F}{P_{IN}}, \tag{10}$$

where η_F is the Faradaic efficiency. The Faradaic efficiency is a measure of the efficiency of electron transfer in the chemical reaction, and is independent of the details of the supplied power and associated losses. We assume that $\eta_F = 1$ in this work.

A key point here is that the efficiency is determined by the product of the operating current density j_{op} and the fixed reaction potential, ΔE. In order to maximise the efficiency, it is necessary to find the optimum operating current density which maximises the current while minimising the current dependent voltage loss, $|V_{IN} - \Delta E|$. To find the optimum operating current density for a given system, we minimise the current density dependent function,

$$f(j) = V_{IN}(j) - \Delta E + V_{OER}(j) + V_{HER}(j) + V_e(j), \tag{11}$$
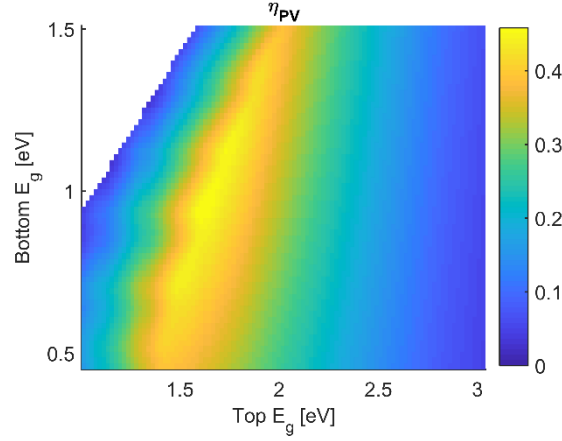
Modelling Ideal tandem solar cells

Figure S1 Thermodynamic limiting efficiencies for tandem solar cells in a 2-terminal configuration

Thermodynamic limiting power conversion efficiencies for tandem solar cells in a 2-terminal configuration as a function of the complementary semiconductor bandgaps.

Modelling Realistic Tandems

The photovoltage of a realistic PV component is given by solving the trancendental solar cell equation,

$$V_{PV}(j) = \frac{k_B T}{e} ln \left(\frac{j_L - j - \left(\frac{V_{PV}(j) - R_S j}{R_{sh}} \right)}{j_0} + 1 \right) - jR_S, \tag{12}$$

and introducing loss parameters to account for non-ideal absorption, non-ideal recombination, and non-ideal diode behaviour. The non-ideal recombination current density is calculated as

$$j_0 = \frac{j_{rad}(E_g)}{ERE} \tag{13}$$

where the external radiative efficiency factor, ERE, quantifies the fraction of the total recombination that can be attributed to ideal, radiative recombination, j_{rad}.

To determine non-ideal photocurrent we calculate realistic absorption spectra, $A(\lambda)$, and define the collection efficiency, f_c, to account for any charge carrier collection losses. The absorption in the Si cell was calculated assuming Lambertian light trapping and no reflection loss, following the work of Green[4], while a bandgap dependent analytical approximation was used to reproduce the shape of the absorption spectra of the top cells. An additional loss factor, f_{Para}, was defined for the top cells to account for parasitic absorption that would reduce the light incident on the bottom cell.

The photocurrent is then given by:

$$j_{L,top} = e f_c \int_{AM1.5g} A_{top}(\lambda) \Phi(\lambda) d\lambda. \tag{14}$$

for the top cell, and

$$j_{L,Si} = ef_c \int_{AM1.5g} A_{Si}(\lambda)\big(1 - A_{top}(\lambda) - A_{para}(\lambda)\big)\Phi(\lambda)d\lambda. \qquad (15)$$

For the bottom silicon cell. Resistive losses due to carrier transport in the semiconductor are introduced through the series resistance term, R_s, and non-ideal diode characteristics are introduced through the shunt resistance, R_{sh}. The series and shunt resistances were modelled using the normalised resistance, r_s, r_{sh} for each cell, defined as

$$r_{s/sh} = R_{s/sh}\, \frac{j_L}{V_{oc}}. \qquad (16)$$

The loss parameters were fitted to reproduce the reported experimental current-voltage curves and solar cell figures of merit in refs [5,6]. Where possible, the parameters for the silicon bottom cell were taken directly from measurements of an integrated back contact (IBC) cell reported by Franklin[7], as this is similar to the bottom cell used in the Perovskite-Si tandem modelled in this work [6]. The experimentally measured recombination current (i.e. the reverse-biased dark current from ref [7]) was used to to calculate ERE for the silicon cell.

Silicon bottom cell

The recombination current for the Si IBC cell was taken from experimental measurements of the reverse biased current[7], and used to calculate the external radiative efficiency factor, ERE.

The absorption in the Si cell was calculated assuming a 400-µm thick c-Si wafer with Lambertian light trapping and no reflection loss, following the work of Green[4]

$$A_{Si} = \frac{1 - \exp(-2\alpha_{Si}W)}{1 - \left(1 - \frac{1}{n_{Si}^2}\right)\exp(-2\alpha_{Si}W)}, \qquad (17)$$

where α_{Si} and n_{Si} are the wavelength dependent absorption coefficient and refractive index of crystalline Si. To account for absorption in the top cell, A_{Si} was multiplied by the transmission of the top cell, T_{Top}, the calculation of which is described below. A collection efficiency, f_c, defined as the fraction of photogenerated carriers that contribute to the current. The light induced current was then calculated by integrating the product of these three terms with the photon flux in the AM1.5g solar spectrum:

$$j_{L,Si} = f_c e \int_{\lambda_{min}}^{\lambda_{max}} A_{Si} T_{Top} \Phi(\lambda)d\lambda \qquad (18)$$

Top Cells

The recombination current was estimated by including the external radiative efficiency factor, ERE, which quantifies the fraction of the total recombination that can be attributed to ideal recombination, given by the blackbody radiation from the cell at room temperature, T = 300K

$$j_0 = Ae \int_{\lambda_{min}}^{\frac{hc}{Eg}} \frac{2\pi c}{\lambda^4}\left(exp\left[\frac{hc}{\lambda k_B T}\right] - 1\right)d\lambda. \qquad (19)$$

Where k_B is the Boltzmann constant, e is the charge on the electron, c is the speed of light, λ is the wavelength of light, and h is Planck's constant. The total, bandgap dependent recombination current can then be calculated as

$$j_r = \frac{i_0(Eg)}{ERE}. \qquad (20)$$

To determine the photocurrent a simple, bandgap dependent, analytical approximation was used to model the shape of the experimentally reported absorption spectra of the top cells [6,5]:

$$A_{Top} = 0.45 \, \text{erf}\left(\frac{\frac{hc}{\lambda}-E_g}{\frac{5k_BT}{e}}\right) + 0.05\,\text{erf}\left(\frac{hc}{\lambda} - E_g\right) + 0.05 \qquad (21)$$

An additional parameter was introduced to include parasitic (below bandgap) absorption in the top cell, f_{Para}:

$$A_{Para} = f_{para} \, \text{erf}\left(\frac{\frac{hc}{\lambda}-E_g}{\frac{7k_BT}{e}}\right) \quad , \frac{hc}{\lambda} < E_g \qquad (22)$$

The transmission through the top cell is then calculated as:

$$T_{Top} = 1 - A_{Para} - A_{Top} \qquad (23)$$

The calculated absorption spectra for all the modelled cells are given in Figure S2 (a) and (c) below.
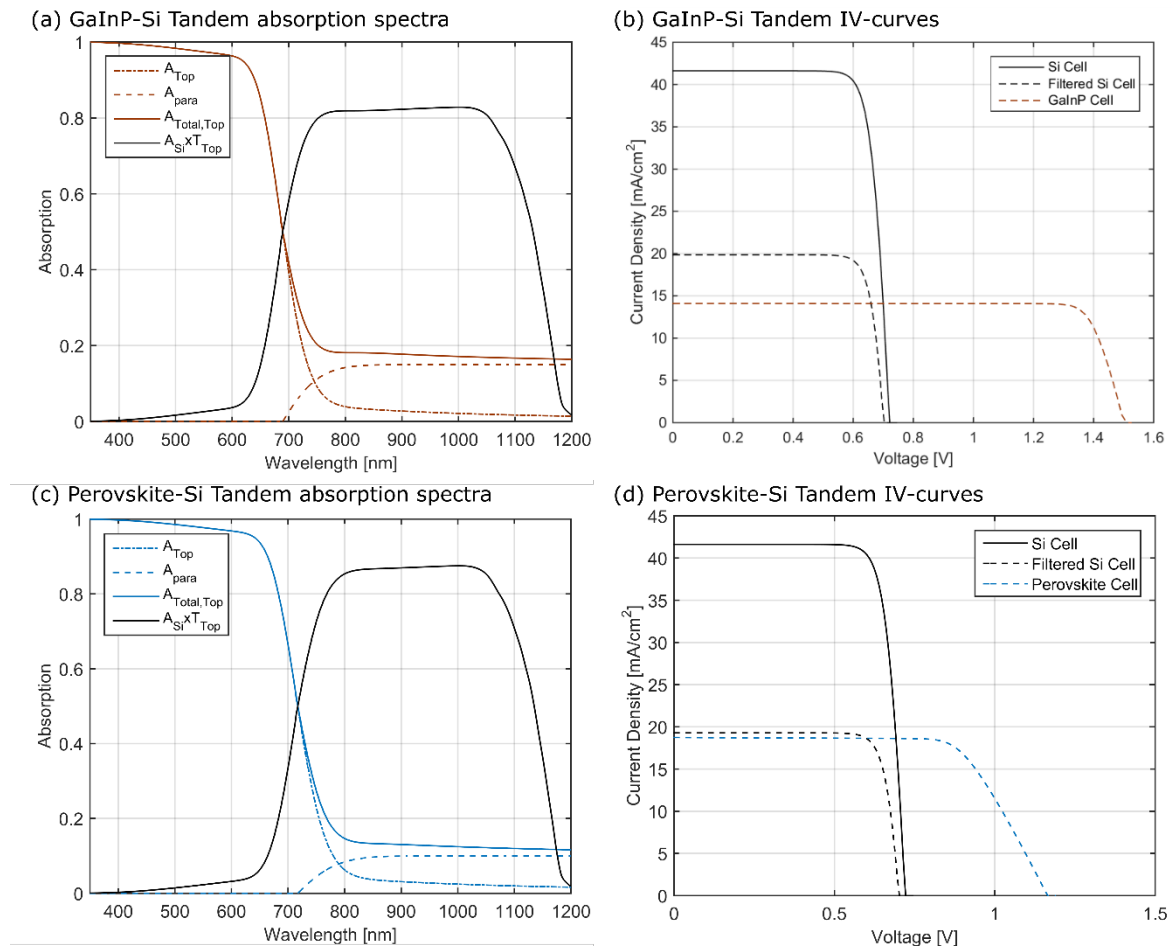

Figure S2 Calculated absorption spectra for (a) GaInP-Si tandems and (c) Perovskite-Si tandems used in this work. Current-voltage curves for (b) GaInP-Si tandems and (d) Perovskite-Si tandems

Fitting Proceedure

The three loss parameters for the Si cell - collection efficiency, f_c, normalied series, r_s, and shunt resistance, r_{sh} - were chosen to give the best fit to the experimentally reported Si IBC solar cell data in ref, including the "Silicon-original" IV-curve in Fig 6(c), and the data for the "IBC cell – Without filter" in Table 1 in ref[6].

Table S1 Calculated figures of merit for the modelled photovoltaic components

	Si	GaInP	PEROVSKITE
BANDGAP [EV]	1.1	1.8	1.73
V$_{OC}$ [V]	0.69	1.47	1.14 V
J$_{SC}$ [mA/cm^2]	41.6	14.0	18.8
FF	84%	88%	72%
SINGLE CELL EFFICIENCY	24.4%	18.3%	15.5%
TANDEM EFFICIENCY (4T)	--	29.9%	26.7%

Once the Si cell parameters were chosen, f_c and f_{Para} for the top cells where chosen to closely match the EQE profiles given in Fig. 6(b) in ref [6]. Once these parameters were fixed, ERE, r_s, and r_{sh} were chosen such that calculated current-voltage curves matched those reported in Fig 6(c), and the figures of merit for the "Perovskite (top cell)" in Table 1 were reproduced. Finally, the parasitic absorption in the top cell was adjusted so that the figures of merit for Si as a bottom cell matched data for the "IBC cell – With filter" in Table 1 in ref [6]. This procedure was repeated for the GaInP top cell, using [5] as a reference. The resulting current-voltage curves are given in Figure S2(b) for the GaInP-Si tandem and (d) for the Perovskite-Si tandem. Calculated figures of merit are given in Table S1.

Effect of illumination intensity

The effect of illumination intensity was investigated by multiplying the standard input spectra (AM1.5g) by a factor: $0.5 < F_{sun} < 1.5$. Calculations were performed for realistic Perovskite-Silicon tandems, with high cost catalysts, for a range of top cell bandgaps in both the coupled and decoupled configuration.

The illumination intensity affects both the voltage and the current of a solar cell: for the current, the dependence is linear, while the voltage has a less sensitive logarithmic dependence. For realistic cells, series and shunt resistance will lead to increasing voltage and current losses respectively as the illumination increased (see eq 14 above). Additionally, the overpotential of the catalysts is also a function of the input current (see Eq 8 above), and increasing current will lead to higher overpotential losses.

Figure S3 shows that the illumination intensity will affect the solar-to-hydrogen efficiency slightly for both decoupled and coupled realistic Perovskite-Silicon solar hydrogen systems. The optimum bandgap for each configuration is largely unaffected by the illumination intensity and both systems have highest efficiency at lower illumination where the shunt, series, and overpotential losses will be lower. The output of the coupled systems are relatively stable with changes in intensity since they are limited by the fixed voltage requirement, and the output voltage is only weakly dependent on the illumination intensity.

It is informative to look at the output current as well as the efficiency when comparing illumination, as the output current determines the amount of hydrogen generated per second. As expected, the output current increases with illumination intensity as the photocurrent increases. In all cases, the decoupled system performs better, and is less sensitive to bandgap and intensity variations than the coupled system.
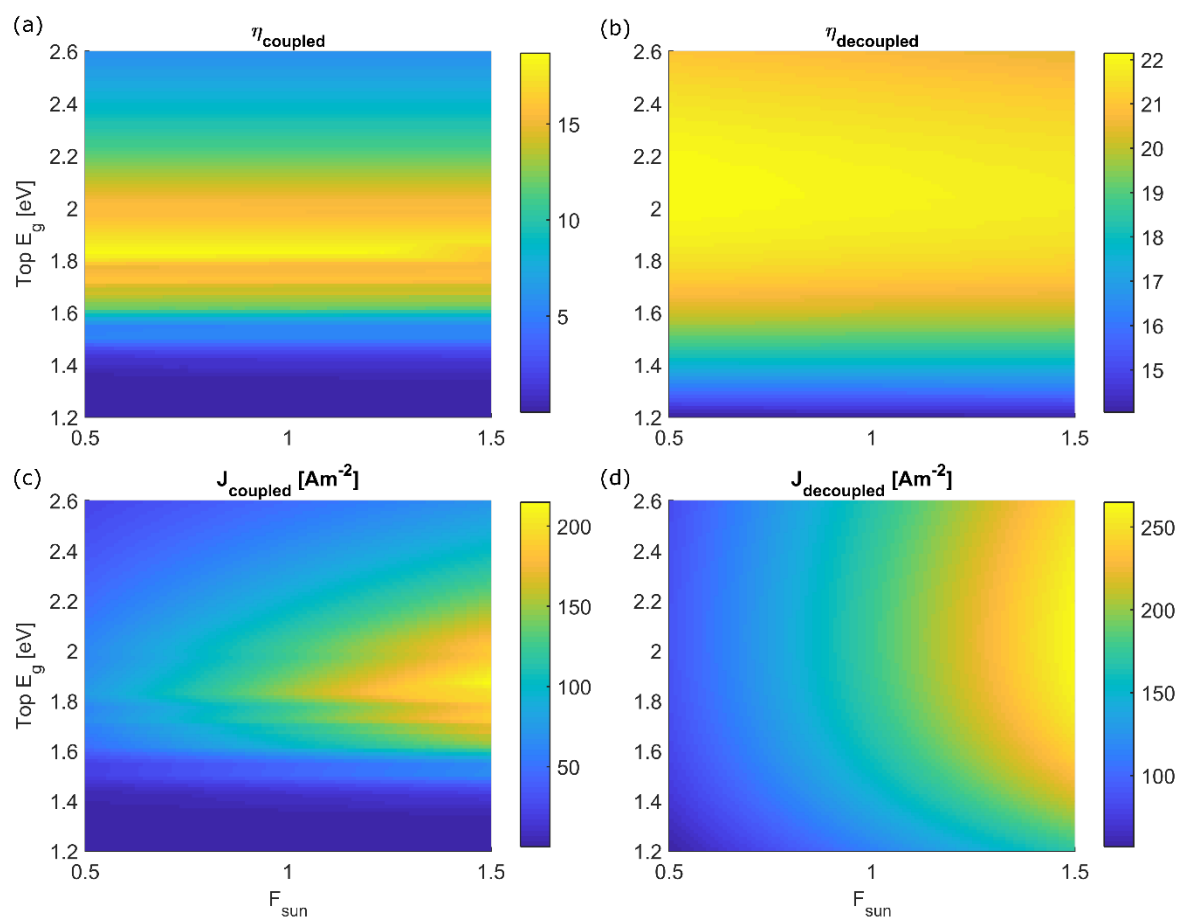

Figure S3 Calculated solar to hydrogen efficiencies for (a) coupled and (b) decoupled Perovskite-Si tandems for different top cell bandgaps, $Top\ E_g$, and illuminations as a fraction of 1-sun illumination, F_{sun}. Calculated output for (c) coupled and (d) decoupled Perovskite-Si tandems for different top cell bandgaps, $Top\ E_g$, and illuminations as a fraction of 1-sun illumination, F_{sun}.

References

(1)   Fountaine, K. T.; Lewerenz, H. J.; Atwater, H. A. Efficiency Limits for Photoelectrochemical Water-Splitting. *Nat. Commun.* **2016**, *7*, 1–9. https://doi.org/10.1038/ncomms13706.

(2)   Shaner, M. R.; Fountaine, K. T.; Lewerenz, H. J. Current-Voltage Characteristics of Coupled Photodiode-Electrocatalyst Devices. *Appl. Phys. Lett.* **2013**, *103* (14). https://doi.org/10.1063/1.4822179.

(3)   Bard, A. J.; Faulkner, L. R. *ELECTROCHEMICAL METHODS Fundamentals and Applications*, 2nd ed.; John Wiley and Sons, Inc.: New York, 1944.

https://doi.org/10.1016/B978-0-12-381373-2.00056-9.

(4)   Green, M. A. Lambertian Light Trapping in Textured Solar Cells and Light-Emitting
        Diodes: Analytical Solutions. *Prog. Photovoltaics Res. Appl.* **2002**, *10* (4), 235–241.
        https://doi.org/10.1002/pip.404.

(5)   Essig, S.; Steiner, M. A.; Allebé, C.; Geisz, J. F.; Paviet-Salomon, B.; Ward, S.;
        Descoeudres, A.; LaSalvia, V.; Barraud, L.; Badel, N.; Faes, A.; Levrat, J.; Despeisse, M.;
        Ballif, C.; Stradins, P.; Young, D. L. Realization of GaInP/Si Dual-Junction Solar Cells
        with 29.8% 1-Sun Efficiency. *IEEE J. Photovoltaics* **2016**, *6* (4), 1012–1019.
        https://doi.org/10.1109/JPHOTOV.2016.2549746.

(6)   Duong, T.; Wu, Y. L.; Shen, H.; Peng, J.; Fu, X.; Jacobs, D.; Wang, E. C.; Kho, T. C.; Fong,
        K. C.; Stocks, M. Franklin, E.; Blakers, A.; Zin, N., McIntosh, K.; Li, W.; White, T. P.;
        Weber, K.; Catchpole, K. R. . Rubidium Multication Perovskite with Optimized
        Bandgap for Perovskite-Silicon Tandem with over 26% Efficiency. *Adv. Energy Mater.*
        2017, *7* (14), 1–11. https://doi.org/10.1002/aenm.201700228.

(7)   F Franklin, E.; Fong, K.; McIntosh, K.; Fell, A.; Blakers, A.; Kho, T.; Walter, D.; Wang, D.;
        Zin, N.; Stocks, M.; Wang, E.; Grant, N.; Wan, Y.; Yang, Y.; Zhang, X.; Feng, Z.;
        Verlinden, P. J. Design, Fabrication and Characterisation of a 24.4% Efficient
        Interdigitated Back Contact Solar Cell. *Prog. Photovoltaics Res. Appl.* **2016**, *24* (4),
        411–427. https://doi.org/10.1002/pip.2556.